Research Article

Nano Research
2020, 13(5): 1472–1478

ISSN 1998-0124 CN 11-5974/O4
https://doi.org/10.1007/s12274-020-2754-4

Pt_3Ag alloy wavy nanowires as highly effective electrocatalysts for ethanol oxidation reaction

Xiaoyang Fu[1], Chengzhang Wan[1], Aixin Zhang[1], Zipeng Zhao[2], Huaixun Huyan[3], Xiaoqing Pan[3,4,5], Shuaijing Du[1], Xiangfeng Duan[1,6] (✉), and Yu Huang[2,6] (✉)

[1] *Department of Chemistry and Biochemistry, University of California, Los Angeles, Los Angeles, California 90095, USA*
[2] *Department of Materials Science and Engineering, University of California, Los Angeles, Los Angeles, California 90095, USA*
[3] *Department of Chemical Engineering and Materials Science, University of California, Irvine, Irvine, California 92697, USA*
[4] *Irvine Materials Research Institute (IMRI), University of California, Irvine, Irvine, California 92697, USA*
[5] *Department of Physics and Astronomy, University of California, Irvine, Irvine, California 92697, USA*
[6] *California Nanosystems Institute, University of California, Los Angeles, Los Angeles, California 90095, USA*

Received: 28 December 2019 / **Revised:** 20 February 2020 / **Accepted:** 10 March 2020

ABSTRACT

Direct ethanol fuel cell (DEFC) has received tremendous research interests because of the more convenient storage and transportation of ethanol vs. compressed hydrogen. However, the electrocatalytic ethanol oxidation reaction typically requires precious metal catalysts and is plagued with relatively high over potential and low mass activity. Here we report the synthesis of Pt_3Ag alloy wavy nanowires via a particle attachment mechanism in a facile solvothermal process. Transmission microscopy studies and elemental analyses show highly wavy nanowire structures with an average diameter of 4.6 ± 1.0 nm and uniform Pt_3Ag alloy formation. Electrocatalytic studies demonstrate that the resulting alloy nanowires can function as highly effective electrocatalysts for ethanol oxidation reactions (EOR) with ultrahigh specific activity of 28.0 mA/cm^2 and mass activity of 6.1 A/mg, far exceeding that of the commercial Pt/carbon samples (1.10 A/mg). The improved electrocatalytic activity may be partly attributed to partial electron transfer from Ag to Pt in the Pt_3Ag alloy, which weakens CO binding and the CO poisoning effect. The one-dimensional nanowire morphology also contributes to favorable charge transport properties that are critical for extracting charge from catalytic active sites to external circuits. The chronoamperometry studies demonstrate considerably improved stability for long term operation compared with the commercial Pt/C samples, making the Pt_3Ag wavy nanowires an attractive electrocatalyst for EOR.

KEYWORDS

platinum, silver, alloy, wavy nanowires, electrocatalysis, ethanol oxidation reaction (EOR)

1 Introduction

Compared with compressed hydrogen, alcohols have higher volumetric energy density and gravimetric energy density if we take the weight of the hydrogen tank into account [1]. In addition, they are also easier and intrinsically safer for storage and transport, making them attractive candidates for fuel cells [1]. Among the various alcohol fuel cells, ethanol has higher volumetric energy and gravimetric energy density than methanol, more importantly it also has the advantage for being much less toxic and produced renewable at lower cost [1]. Specifically, the alkaline direct ethanol fuel cell (ADEFC) is attracting increasing research interests recently [2]. In alkaline environment, the kinetics of cathode oxygen reduction reaction (ORR) becomes more favorable, which provides us with the choices of cheaper ORR electrocatalysts, such as AlN [3], ZrN [4] and many non-precious metal-based nanomaterials [5]. The reversed direction of the electro-osmotic drag also lowers the ethanol crossover in the cell, leading to higher efficiency [2]. The disadvantage of voltage drop caused by the CO_3^{2-} formation can be alleviated by changing electrolyte periodically or increasing operation temperature [6, 7]. However, the ethanol oxidation reaction (EOR) is kinetically much more difficult compared with the hydrogen oxidation reaction (HOR), and often requires precious metal-based electrocatalysts. Currently, Pt [8] and Pd [9] are the most widely studied catalyst materials for EOR, which are still limited by relatively high overpotential, undesirable poisoning effect and low mass activity. Therefore, developing noble metal based electrocatalysts with high mass activity (MA) (defined as electrocatalytic performance normalized by the mass loading of the noble metal) is of great importance for cost-effective direct ethanol fuel cells.

In general, the mass activity of an electrocatalyst is determined by the product of the specific activity (SA) and electrochemical active surface area (ECSA). To enhance the SA, the surface modification remains to be the most common way, including creating alloys and hybrids materials. For example, Ru [10, 11], Ni [12] or $Ni(OH)_2$ [13, 14] have been employed as highly oxophilic components to modify Pt or Pd and facilitate the formation of surficial –OH group, which is beneficial for the removal of the carbonaceous species on the nearby noble metal sites via the Langmuir–Hinshelwood mechanism.

Ag has also been suggested as a beneficial component to modify Pt and has received tremendous research interests for

Address correspondence to Yu Huang, yhuang@seas.ucla.edu; Xiangfeng Duan, xduan@chem.ucla.edu

several reasons. Ag itself has the highest specific conductivity among all metals, which is intrinsically beneficial for electrocatalysis since charge transport is essential for electrocatalysis [15]. Additionally, Ag not only intrinsically binds weakly to CO as shown from the volcano plot (like Cu and Au from the same group) [16], but also helps adjust the d-band structure and enrich the local electron density around Pt upon alloying, which lowers the electron donation from CO to Pt and thus potentially weakens CO chemisorption and mitigates undesirable poisoning effect [17, 18]. Very recently, theoretical study suggested that the Pt_3Ag alloy with (111) crystal surface can facilitate the C–C bond cleavage during ethanol oxidation reaction [19], thus delivering a higher efficiency of utilizing ethanol as a fuel. Therefore, it is expected the Pt_3Ag alloy may be a good candidate for electrocatalytic ethanol oxidation reaction with improved SA.

Apart from increasing the SA, the enhancement of ECSA is also essential for enhancing the overall MA. To this end, the use of ultrafine nanostructures is important. However, ultrafine nanoparticles are usually not very stable under aggressive electrochemical reaction conditions due to the physical movement/aggregation and Oswald ripening processes. The one-dimensional (1D) nanowires is less mobile, more stable and less subjected to these drawbacks [20]. Thus, ultrathin nanowires represents an attractive class of electrocatalysts that can deliver ultrahigh ECSA [20, 21]. For the nanowires with wavy morphologies (wavy nanowires), the wavy surface with rich surface defects may also provide additional catalytic hotspots for further improved activity [22, 23]. Lastly, the 1D structure is also believed to have an intrinsic advantage to facilitate charge transport for more efficient utilization all available catalytic sites.

Here we report the synthesis of the Pt_3Ag wavy nanowires through a particle attachment mechanism in a facile solvothermal process. Transmission microscopy studies and elemental analyses reveal highly wavy nanowire structure with an average diameter of 4.6 ± 1.0 nm and uniform Pt_3Ag alloy formation. Electrocatalytic studies demonstrate that the alloy wavy nanowires may function as high effective electrocatalysts for EOR with an ultrahigh SA (28.0 mA/cm^2) and a highest mass activity of 6.1 A/mg, far exceeding that of the commercial Pt/carbon samples (1.10 A/mg).

2 Experimental

2.1 Chemicals

Potassium tetrachloroplatinate(IV) (K_2PtCl_4, 98%), silver nitrate ($AgNO_3$, analytical grade), polyvinylpyrrolidone (PVP, M_W ~ 55,000), concentrated ammonium hydroxide ($NH_3{\cdot}H_2O$, 28.0%–30.0%), sodium borohydride ($NaBH_4$), ethanol, acetone, ethylene glycol (EG, anhydrous, 99.8%) and the commercial platinum carbon (20%) were all used as received without further purification.

2.2 Synthesis of Pt_3Ag wavy nanowires

160 mg PVP were dissolved into 4 mL EG after ultrasonication at first. And 0.018 mmol K_2PtCl_4 and 0.006 mmol $AgNO_3$ were dissolved in 1.0 mL and 0.25 mL deionized (DI) water, respectively. Then we uniformly mixed the aqueous solution of the Pt and Ag precursors with the EG solution of PVP in turn. The vial was then heated at 210 °C for 4 h. After cooling to room temperature, we added 0.7 mL concentrated ammonia water and 2 mL aqueous solution of $NaBH_4$ (5.0 mg) for cleaning. After 1 h, the products were collected via centrifugation after the addition of acetone and then washed with water for 2 times and ethanol for 2 times. Finally they were dispersed in ethanol for further study.

2.3 Structural characterizations

The X-ray diffraction (XRD) was tested on a Panalytical X'Pert Pro X-ray Powder Diffractometer with Cu-Kα radiation after drop-casting the ethanol dispersion of Pt_3Ag wavy nanowires onto the glassy substrate and dried under room temperature. X-ray photoelectron spectroscopy (XPS) tests were carried out with Kratos AXIS Ultra DLD spectrometer after drop-casting ethanol dispersion of the sample on the silicon substrate and then dried. Transmission electron microscopy (TEM) images were carried out on an FEI T12 transmission electron microscope operated at 120 kV. High resolution TEM (HRTEM) images were taken on FEI Titan transmission electron microscope operated at 300 kV. The scanning TEM (STEM) image and energy dispersive X-ray spectroscopy (EDS) mapping were carried out on Joel Jem-300CF (Grand Arm) operated at 300 kV. The samples were prepared by dropping ethanol dispersion of the sample onto the carbon-coated copper TEM grids. The Pt loading of Pt_3Ag wavy nanowires on the glassy carbon electrode (GCE) was determined by the inductively coupled plasma-atomic emission spectroscopy (ICP-AES).

2.4 Electrochemical measurements

All the electrochemical studies were carried out via a three-electrode cell system. The working electrode was a GCE with a geometry area of 0.196 cm^2 and the counter electrode was a Pt wire. We used Hg/HgO (1 M KOH) as the reference electrode for electrochemical test in alkaline media and Ag/AgCl as the reference electrode in acidic media. All the potential were converted against RHE. In order to fabrication the working electrode, the Pt_3Ag wavy nanowires were homogeneously dispersed in EtOH after sonication and 10.0 μL of the ink was drop-cast onto the surface of the electrode surface and dried at room temperature. The Pt loading of our nanowires on the electrode determined from ICP-AES was 2.10 μg (10.7 μg/cm^2 as normalized by the geometric area of the GCE).

To activate the electrocatalysts, cyclic voltammetry (CV) tests were performed in Ar-saturated 0.5 M H_2SO_4 electrolyte with a scan rate of 50 mV/s ranging from 0.05 to 1.0 V vs. RHE. The electrochemical active surface area determined from hydrogen under potential deposition ($ECSA_{Hupd}$) was calculated by integrating hydrogen desorption charge using the constant of 210 μC/cm^2 for the hydrogen monolayer on platinum. Electrocatalytical EOR tests were carried out in Ar-saturated 1 M KOH + 1 M EtOH electrolyte with potential scan rate of 50 mV/s in the range from 0.05 to 1.1 V vs. RHE. To test the long term performance of the electrocatalysts, the chronoamperometry (CA) tests were carried out at 0.72 V vs. RHE for 6,000 s. Commercial platinum carbon was used as control and 1.00 mg commercial Pt/C (20%) was mixed with 0.99 mL ethanol and 10.0 μL Nafion (5 wt.%) to prepare the ink after ultrasonication. And 5.0 μL of the Pt/C catalyst ink was drop-cast onto the GCE and dried to ensure a platinum loading of 1.0 μg (5.1 μg/cm^2) on the working electrode to ensure similar background current during CV scan. For the CA tests, the Pt-loading of Pt/C is 2.0 μg (10.2 μg/cm^2) by drop casting 10.0 μL of the Pt/C catalyst ink. All the electrochemical tests were carried out under the same conditions for the controlled sample of commercial Pt/C (20%).

3 Results and discussion

3.1 Characterizations of Pt_3Ag wavy nanowires

The morphologies of the wavy Pt_3Ag nanowires were studied by

TEM. TEM image clearly demonstrates ultrafine wavy nanowire geometry with diameters mainly in the range of ~ 3–6 nm and lengths exceeding 300 nm (Fig. 1(a)). The high-resolution TEM shows clearly resolved lattice fringes with a lattice spacing of 0.231 nm (Fig. 1(b) and inset). This value falls between the lattice spacing of the (111) crystal planes of face center cubic (FCC) Pt (0.227 nm) and FCC Ag (0.236 nm), indicating the formation of FCC alloys between Pt and Ag, which is also generally consistent with previous reports about the alloys between platinum and silver [24, 25]. Similar to the previously reported wavy nanowires, there are also apparently many surface defects, which may function as the catalytic active sites and contribute to the electrocatalytic performances according to the previous reports about wavy nanowires [22, 23]. More importantly, the exposed (111) crystal plane of Pt_3Ag is also believed to help with C–C bond cleavage during EOR based on the previous theoretical study [19]. A statistical analysis of the diameters of the wavy nanowires reveals an average diameter of 4.6 ± 1.0 nm (Fig. 1(c)). Such small diameter is beneficial for boosting the ECSA.

To evaluate the alloy formation and elemental distribution within the wavy nanowires, we have conducted STEM studies and elemental mapping statues using EDS (Figs. 1(d)–1(f)). The EDS mapping demonstrates that uniform distributions of platinum and silver throughout the wavy nanowires, confirming the formation of uniform alloy. The ratio of Pt:Ag determined from EDS analysis is 2.76:1 as shown in Fig. S1 in Electronic Supplementary Material (ESM), which also agrees well with the results from ICP-AES (2.83:1) and the feed ratio of the precursors (3:1), further confirming the composition of the alloy wavy nanowires.

Figure 1(g) shows the XRD pattern of the Pt_3Ag wavy nanowires sample. Compared with the standard XRD pattern of the FCC silver (JCPDS No. 04-0783) and FCC platinum (JCPDS No. 04-0802) whose characteristic peaks are attributed to the (111), (200), (220), (311) and (222) crystal planes, the Pt_3Ag nanowires also show the same set of peaks attributed to (111), (200), (220), (311) and (222) crystal planes positioned exactly between those of Pt and Ag, further confirming the formation of uniform alloys, which is also consistent with the observations from HRTEM and EDS mapping. By applying Scherrer's equation for these peaks, the size of the crystallites is estimated to be 4.3 nm, which generally agrees with the observations from TEM.

In Figs. 1(h) and 1(i), the XPS results demonstrates the composition and valence of the surface platinum and silver species in Pt_3Ag nanowires. The peaks at the binding energies (BE) of 71.0 and 74.4 eV correspond to the $4f_{7/2}$ and $4f_{5/2}$ of the Pt(0), respectively [24, 25]. The peaks at the BE of 71.9 and 75.3 eV correspond to the $4f7_{/2}$ and $4f_{5/2}$ of the Pt(II) [24, 25] while the peaks at the 73.4 and 77.3 eV correspond to the $4f_{7/2}$ and $4f_{5/2}$ of the Pt(IV) species [26]. These oxidized Pt species might be attributed to the oxidized surficial Pt in air or the unreacted precursor. The peak area ratio of $4f_{7/2}$ and $4f_{5/2}$

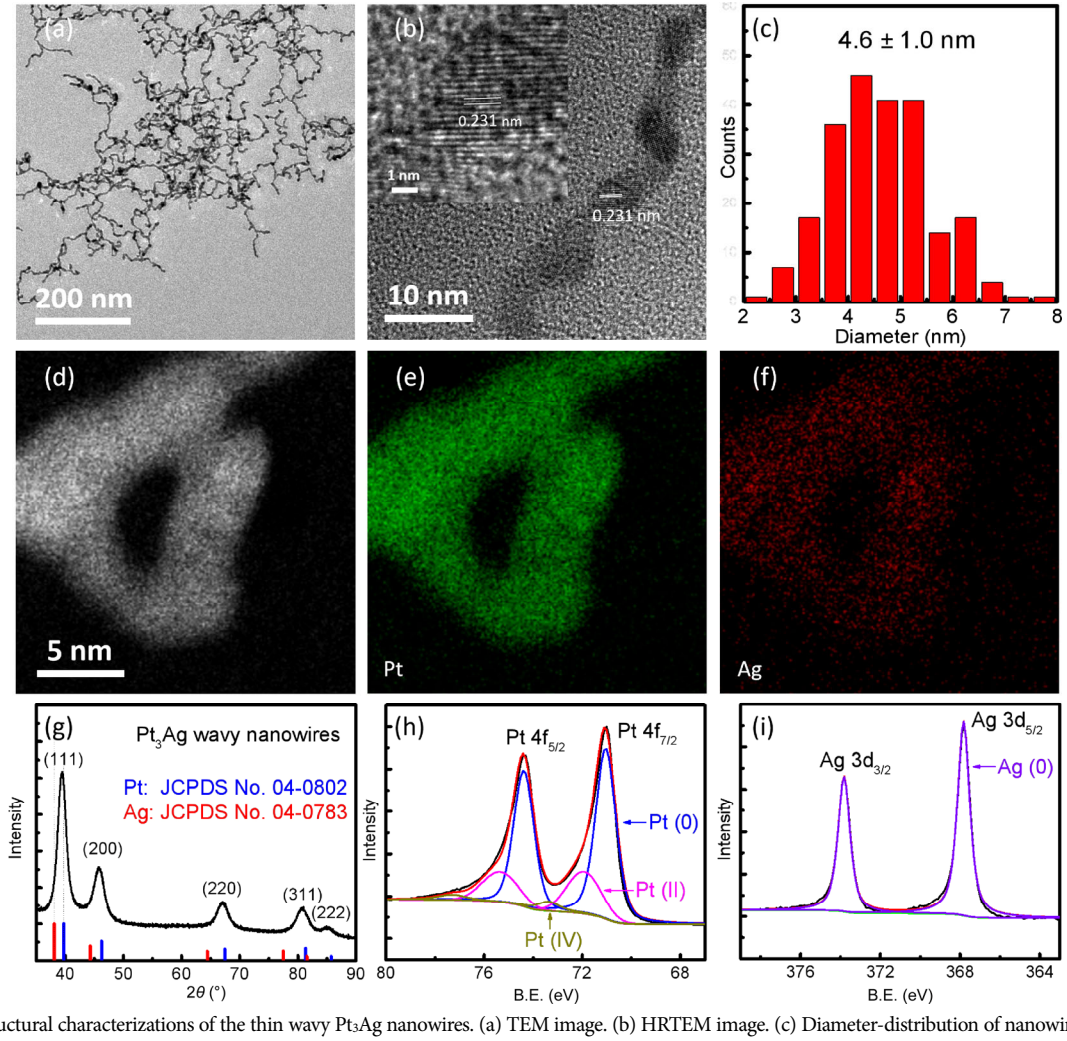

Figure 1 Structural characterizations of the thin wavy Pt_3Ag nanowires. (a) TEM image. (b) HRTEM image. (c) Diameter-distribution of nanowires. (d) Selected area for EDS mapping. (e) EDS mapping of Pt element. (f) EDS mapping of Ag element. (g) XRD characterization. (h) XPS characterization for Pt element. (i) XPS characterization for Ag element.

follows the theoretical value of 4:3 for all split peaks of Pt(0), Pt(II) and Pt(IV) and the content of Pt(0) is calculated as 70.2% based on the peak area. For silver, the peaks at the BE of 367.8 and 373.8 eV correspond to the $3d_{5/2}$ and $3d_{3/2}$ of the Ag(0) following the theoretical value of 3:2, The absence of other split peaks indicates that the silver exists predominately as metallic Ag(0).

We also find that the BE for the Pt 4f orbits are comparably lower than those of commercial Pt/C as shown in Fig. S2 in the ESM with Pt(0) $4f_{7/2}$ shifted from 71.3 to 71.0 eV and Pt(0) $4f_{5/2}$ shifted from 74.6 to 74.4 eV upon alloying with silver, indicating the electronic states of Pt are adjusted due to the electron donation from silver (electronegativity: 1.93) to platinum (electronegativity: 2.28). It has been proposed that the negatively shifted BE indicates enriched electron density of Pt, which could weaken the interaction with lone electron pair of CO and other carbonaceous species, and thus lowers the binding and poisoning effect [18, 27]. Accordingly, silver also has higher BE when compared with pure Ag NWs with Ag(0) $3d_{5/2}$ shifted from 367.4 to 367.8 eV and Ag(0) $3d_{3/2}$ shifted from 373.4 to 373.8 eV, which further confirms the electrons transfer from Ag to Pt [28].

In our synthesis of the Pt_3Ag wavy nanowires, EG works as the reducing agent under high temperature while PVP works as the template agent to help forming wavy nanowires via the particle attachment mechanism. Similar synthetic system for wavy nanowire growth has also been reported with PVP as the template agent previously [23]. In addition, PVP will also help with the exposure of the (111) crystal plane of the noble metals, which is important for many catalytic reactions [29, 30] including EOR [19].

To further reveal the growth mechanism, we have also taken TEM pictures of the products collected at the different reaction intervals (Fig. 2). At t = 1 min, there are lots of tiny crystallites (~ 2 nm) formation. As the reaction time goes, there are short nanorods beginning to form (t = 5 and 10 min), followed by the formation of longer nanowires (t = 20, 30 and 60 min). This observation also agrees with the previous literature about the particle attachment mechanism for wavy nanowire growths [23, 24].

3.2 Electrocatalytic ethanol oxidation reaction

We have first conducted electrochemical CV to determine the $ECSA_{Hupd}$ of the Pt_3Ag wavy nanowire catalysts (Fig. 3(a)). In the 0.5 M H_2SO_4 electrolyte, the forward scan demonstrates the characteristic hydrogen desorption region while the

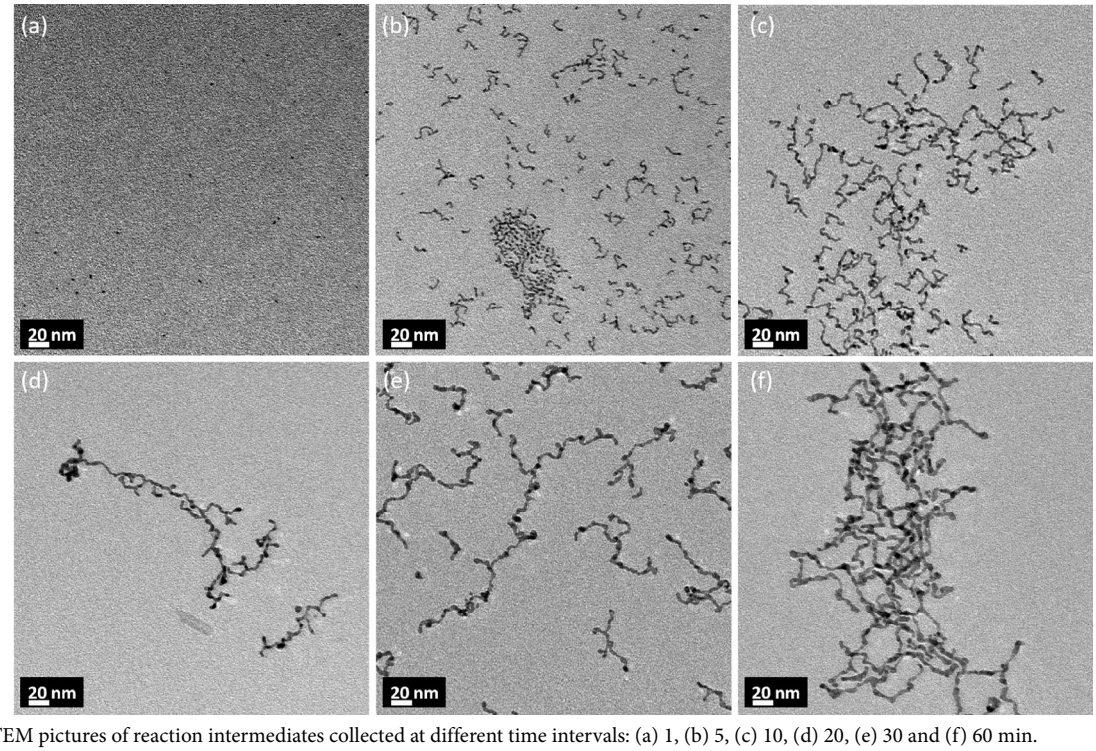

Figure 2 TEM pictures of reaction intermediates collected at different time intervals: (a) 1, (b) 5, (c) 10, (d) 20, (e) 30 and (f) 60 min.

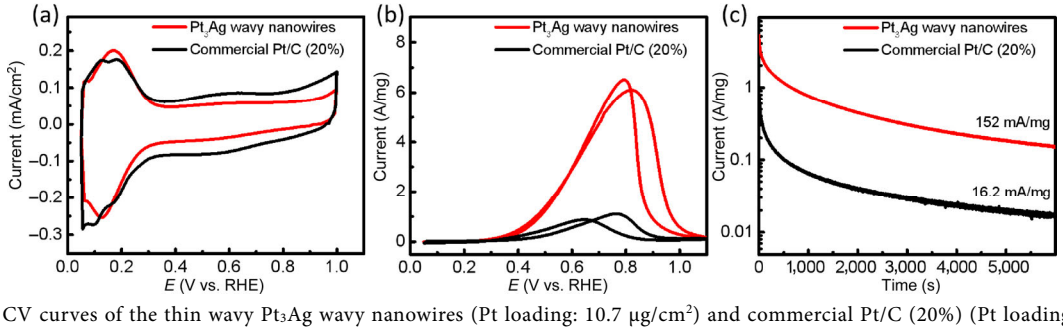

Figure 3 (a) CV curves of the thin wavy Pt_3Ag wavy nanowires (Pt loading: 10.7 μg/cm^2) and commercial Pt/C (20%) (Pt loading: 5.1 μg/cm^2) electrocatalysts in 1 M KOH electrolyte at scan rate of 50 mV/s. (b) Mass-normalized CV curves of the thin wavy Pt_3Ag wavy nanowires and commercial Pt/C (20%) electrocatalysts in 1 M KOH + 1 M EtOH electrolyte at scan rate of 50 mV/s. (c) Chronoamperometry results of the thin wavy Pt_3Ag wavy nanowires (Pt loading: 10.7 μg/cm^2) and commercial Pt/C (20%) (Pt loading: 10.2 μg/cm^2) electrocatalysts in 1 M KOH + 1 M EtOH electrolyte at 0.72 V vs. RHE.

reverse scan exhibits the characteristic hydrogen adsorption region. The $ECSA_{Hupd}$ was calculated to be 21.8 m^2/g by using the constant of 210 $\mu C/cm^2$ for the hydrogen monolayer. While the $ECSA_{Hupd}$ of commercial platinum carbon was calculated to be 37.5 m^2/g. The regions corresponding to oxygen desorption and adsorption were very weak since it is not a highly favorable process in acidic media compared with alkaline media.

The theoretical surface area ($ECSA_{Geo}$) for 1D Pt nanowires with average diameter of 4.6 nm is expected to be ~ 40.5 m^2/g by using the geometrical model of thin and long circular cylinder with only lateral area taken into consideration. The smaller ECSA observed in experiments might be attributed to the introduction of Ag on the surface, which is inactive towards the hydrogen underpotential deposition and may partially block the Pt sites [24].

The catalytic activity of the Pt_3Ag nanowires for EOR was carried out in the electrolyte of 1 M KOH and 1 M ethanol (Fig. 3(b)). The forward scan demonstrates a strong current peak at the potential of 0.81 V vs. RHE, corresponding to the oxidation of ethanol with a peak mass activity of 6.1 A/mg. This mass activity is not only 5.5-fold higher than the commercial Pt/C (20%) (1.10 A/mg), but also higher than those of the most previously reported Pt and Pd-based electrocatalysts as shown in Fig. 4(a) (single atom Ni-Pt NWs [21], core–shell $Pt_{56}Cu_{28}Ni_{16}$ tetrahedral [31], $Pt_{75.4}Cu_{24.6}$/RGO [32], $PtPd_3$/rGO/GC [33], Pd/$Ni(OH)_2$/RGO [13] and Pd Aerogel [34]), indicating a great utilization efficiency of the noble metal. In addition, the Pt_3Ag wavy nanowire electrocatalysts also have a more negative shifted onset over-potential (defined as the over-potential required to reach a MA of 0.1 A/mg according to the previous literature [21]) at 0.30 V when compared with the commercial Pt/C (20%) at 0.41 V, suggesting our alloy nanowires also have lower activation barrier for ethanol oxidation reaction.

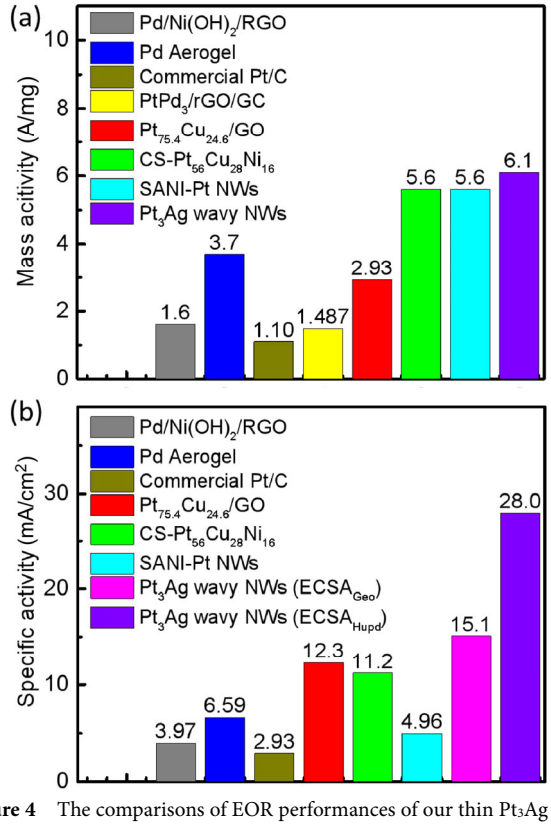

Figure 4 The comparisons of EOR performances of our thin Pt_3Ag alloy wavy nanowires with the previously reported Pt and Pd-based electrocatalysts tested in alkaline media in terms of: (a) mass activity and (b) specific activity.

The specific activity is calculated as 28.0 mA/cm^2 based on the $ECSA_{Hupd}$. Considering that the $ECSA_{Hupd}$ may be underestimated, we may calculate the SA as 15.1 mA/cm^2 by using the geometrical surface area ($ECSA_{Geo}$ ~ 40.5 m^2/g), which is still much higher than most of the previous literatures as shown in Fig. 4(b) (single atom Ni-Pt NWs [21], core–shell $Pt_{56}Cu_{28}Ni_{16}$ tetrahedron [31], $Pt_{75.4}Cu_{24.6}$/RGO [32], Pd/$Ni(OH)_2$/RGO [13] and Pd Aerogel [34]). Such high SA might be attributed to the formation of the Pt_3Ag alloy since the introduction of silver alters the band structure of platinum and lowers the electron donation with CO and other carbonaceous species thus mitigates the binding and the poisoning effect [17], in addition to that Ag also binds very weakly towards CO. Finally according to the recent theoretical studies, the (111) crystal plane of Pt_3Ag alloy can also help cleaving the C–C bond during ethanol oxidation reaction [19], to ensure a more efficient utilization of the energy in ethanol. Therefore, we can tentatively conclude that the ultrahigh mass activity of the Pt_3Ag wavy nanowires largely arises from the ultrahigh SA since the ECSA of the wavy nanowire is moderate due to the relatively thick diameter compared with the previously reported ultrathin nanowires.

In the reverse scan, the anodic peak has a negative potential shift and slightly higher peak current compared with those in the forward scan. However, this reverse scan peak should be no longer attributed to the oxidation of the residue carbonaceous species [35, 36] after the previous forward scan and the I_F/I_R ratio should not be a criterion to evaluate the CO-tolerance ability of the electrocatalyst [37]. Instead, according to the most recent literature on Pt electrocatalyst, during the forward scan, the rate-determining-step (RDS) is the water dissociation step; while during the reverse scan, the Pt is partially oxidized at high potential and the RDS becomes the alcohol dehydrogenation step because of the oxygenated Pt surface, leading to different peak potential and peak current [35, 37].

For our electrocatalyst, it is noted that during the CVs in alkaline electrolyte (without ethanol), our Pt_3Ag nanowires have much less reactivity to oxygen adsorption and desorption compared with the commercial Pt/C (Fig. S3 in the ESM), indicating that it is comparably less susceptible to surface oxide formation during the forward scan and more easily to recover during the backward scan. As a result, the backward scan would be less impacted by oxygenated Pt surfaces after the forward scan. Therefore, the backward scan exhibits a more similarly high current and more similar peak position to those of the forward scan (I_F/I_R = 0.94, ΔE_P = 0.02 V). In comparison, commercial Pt/C has much higher tendency to form a layer of surficial oxide, as indicated by CV in alkaline media, causing the backward scan to go into the alternate pathways and a more evident change in the peak potential and peak current during the backward scan (I_F/I_R = 1.26, ΔE_P = 0.13 V). These similar phenomena and explanations have also been reported with PtNi electrocatalysts before [38].

Finally, the chronoamperometry tests (Fig. 3(c)) were carried out to evaluate the long term performance of the Pt_3Ag wavy nanowire electrocatalyst. The Pt_3Ag wavy nanowire can maintain a current of 152 mA/mg at 0.72 V vs. RHE after 6,000 s. In sharp contrast, the commercial Pt/C only maintains a mass activity of 16.2 mA/mg at 0.72 V vs. RHE after 6,000 s, indicating that Pt_3Ag nanowires has much improved long term performance when compared with the commercial Pt/C. The Pt_3Ag nanowires demonstrate much higher stability and mass activity, which can be mainly attributed to the introduction of Ag to enrich the electron density which weakens the chemisorption of the carbonaceous species [17, 39], and the relatively higher stability of the 1D nanowires under harsh electrochemical

conditions compared (less mobile and less aggregation) with its zero-dimensional (0D) counterparts [20]. Meanwhile, we also find that the catalytic activity can be generally recovered after 25 cycles of CV scanning after each CA test. For example, after 10 rounds of repeated CA tests, the nanowires still maintain a high mass activity of 112 mA/mg (Fig. S4 in the ESM).

4 Conclusion

In summary, we have successfully synthesized Pt_3Ag wavy nanowires via a particle attachment mechanism in a facile solvothermal process. The resulting Pt_3Ag wavy nanowires can function as highly effective EOR electrocatalysts with an extraordinary specific activity of 28.0 mA/cm^2 and an ultrahigh mass activity of 6.1 A/mg, considerably higher than most of the previously reported Pt and Pd-based electrocatalysts in alkaline media, which is largely attributed to the formation of Pt-Ag alloy and electron transfer from Ag to Pt. Furthermore, the Pt_3Ag wavy nanowires also show significantly improved stability, and thus can promise a highly effective electrocatalyst for EOR.

Acknowledgements

X. F. D. acknowledges support from National Science Foundation award 1800580. Y. H. acknowledges support from Office of Naval Research grant N000141812155. X. Q. P. acknowledge the support from the National Science Foundation award DMR-1506535. HAADF imaging and EDS mapping were carried out using the JEOL Grand ARM in the Irvine Materials Research Institute at the University of California, Irvine.

Electronic Supplementary Material: Supplementary material (EDS spectrum of Pt_3Ag alloy wavy nanowires, XPS of Pt/C, CV activation in alkaline media, and long term CA test (10 cycles of 6,000 s) of the electrocatalysts) is available in the online version of this article at https://doi.org/10.1007/s12274-020-2754-4.

References

[1] Joghee, P.; Malik, J. N.; Pylypenko, S.; O'Hayre, R. A review on direct methanol fuel cells—In the perspective of energy and sustainability. *MRS Energy Sustain.* **2015**, *2*, E3.

[2] Yu, E. H.; Krewer, U.; Scott, K. Principles and materials aspects of direct alkaline alcohol fuel cells. *Energies* **2010**, *3*, 1499–1528.

[3] Lei, M.; Wang, J.; Li, J. R.; Wang, Y. G.; Tang, H. L.; Wang, W. J. Emerging methanol-tolerant AlN nanowire oxygen reduction electrocatalyst for alkaline direct methanol fuel cell. *Sci. Rep.* **2014**, *4*, 6013.

[4] Yuan, Y.; Wang, J. C.; Adimi, S.; Shen, H. J.; Thomas, T.; Ma, R. G.; Attfield, J. P.; Yang, M. H. Zirconium nitride catalysts surpass platinum for oxygen reduction. *Nat. Mater.* **2020**, *19*, 282–286.

[5] Wang, D. W.; Su, D. S. Heterogeneous nanocarbon materials for oxygen reduction reaction. *Energy Environ. Sci.* **2014**, *7*, 576–591.

[6] Wang, Y.; Li, L.; Hu, L.; Zhuang, L.; Lu, J. T.; Xu, B. Q. A feasibility analysis for alkaline membrane direct methanol fuel cell: Thermodynamic disadvantages versus kinetic advantages. *Electrochem. Commun.* **2003**, *5*, 662–666.

[7] Cifrain, M.; Kordesch, K. V. Advances, aging mechanism and lifetime in AFCs with circulating electrolytes. *J. Power Sources* **2004**, *127*, 234–242.

[8] Zhang, B. W.; Yang, H. L.; Wang, Y. X.; Dou, S. X.; Liu, H. K. A comprehensive review on controlling surface composition of Pt-based bimetallic electrocatalysts. *Adv. Energy Mater.* **2018**, *8*, 1703597.

[9] Zhang, L. L.; Chang, Q. W.; Chen, H. M.; Shao, M. H. Recent advances in palladium-based electrocatalysts for fuel cell reactions and hydrogen evolution reaction. *Nano Energy* **2016**, *29*, 198–219.

[10] Xu, C. X.; Wang, L.; Mu, X. L.; Ding, Y. Nanoporous PtRu alloys for electrocatalysis. *Langmuir* **2010**, *26*, 7437–7443.

[11] Zhao, S. L.; Yin, H. J.; Du, L.; Yin, G. P.; Tang, Z. Y.; Liu, S. Q. Three dimensional N-doped graphene/PtRu nanoparticle hybrids as high performance anode for direct methanol fuel cells. *J. Mater. Chem. A* **2014**, *2*, 3719–3724.

[12] Jiang, Q.; Jiang, L. H.; Wang, S. L.; Qi, J.; Sun, G. Q. A highly active PtNi/C electrocatalyst for methanol electro-oxidation in alkaline media. *Catal. Commun.* **2010**, *12*, 67–70.

[13] Huang, W. J.; Ma, X. Y.; Wang, H.; Feng, R. F.; Zhou, J. G.; Duchesne, P. N.; Zhang, P.; Chen, F. J.; Han, N.; Zhao, F. P. et al. Promoting effect of $Ni(OH)_2$ on palladium nanocrystals leads to greatly improved operation durability for electrocatalytic ethanol oxidation in alkaline solution. *Adv. Mater.* **2017**, *29*, 1703057.

[14] Huang, W. J.; Wang, H. T.; Zhou, J. G.; Wang, J.; Duchesne, P. N.; Muir, D.; Zhang, P.; Han, N.; Zhao, F. P.; Zeng, M. et al. Highly active and durable methanol oxidation electrocatalyst based on the synergy of platinum–nickel hydroxide–graphene. *Nat. Commun.* **2015**, *6*, 10035.

[15] Zhao, X.; Zhang, H. T.; Yan, Y.; Cao, J. H.; Li, X. Q.; Zhou, S. M.; Peng, Z. M.; Zeng, J. Engineering the electrical conductivity of lamellar silver-doped cobalt(II) selenide nanobelts for enhanced oxygen evolution. *Angew. Chem., Int. Ed.* **2017**, *56*, 328–332.

[16] Kuhl, K. P.; Hatsukade, T.; Cave, E. R.; Abram, D. N.; Kibsgaard, J.; Jaramillo, T. F. Electrocatalytic conversion of carbon dioxide to methane and methanol on transition metal surfaces. *J. Am. Chem. Soc.* **2014**, *136*, 14107–14113.

[17] Shang, C. S.; Guo, Y. X.; Wang, E. K. Integration of two-dimensional morphology and porous surfaces to boost methanol electrooxidation performances of PtAg alloy nanomaterials. *Nano Res.* **2018**, *11*, 6375–6383.

[18] Yang, J.; Ying, J. Y. Nanocomposites of Ag_2S and noble metals. *Angew. Chem., Int. Ed.* **2011**, *50*, 4637–4643.

[19] Monyoncho, E. A.; Steinmann, S. N.; Sautet, P.; Baranova, E. A.; Michel, C. Computational screening for selective catalysts: Cleaving the C–C bond during ethanol electro-oxidation reaction. *Electrochim. Acta* **2018**, *274*, 274–278.

[20] Li, M. F.; Zhao, Z. P.; Cheng, T.; Fortunelli, A.; Chen, C. Y.; Yu, R.; Zhang, Q. H.; Gu, L.; Merinov, B. V.; Lin, Z. Y. et al. Ultrafine jagged platinum nanowires enable ultrahigh mass activity for the oxygen reduction reaction. *Science* **2016**, *354*, 1414–1419.

[21] Li, M. F.; Duanmu, K.; Wan, C. Z.; Cheng, T.; Zhang, L.; Dai, S.; Chen, W. X.; Zhao, Z. P.; Li, P.; Fei, H. L. et al. Single-atom tailoring of platinum nanocatalysts for high-performance multifunctional electrocatalysis. *Nat. Catal.* **2019**, *2*, 495–503.

[22] Fu, X. Y.; Zhao, Z. P.; Wan, C. Z.; Wang, Y. L.; Fan, Z.; Song, F.; Cao, B. C.; Li, M. F.; Xue, W.; Huang, Y. et al. Ultrathin wavy Rh nanowires as highly effective electrocatalysts for methanol oxidation reaction with ultrahigh ECSA. *Nano Res.* **2019**, *12*, 211–215.

[23] Huang, X. Q.; Zhao, Z. P.; Chen, Y.; Chiu, C. Y.; Ruan, L. Y.; Liu, Y.; Li, M. F.; Duan, X. F.; Huang, Y. High density catalytic hot spots in ultrafine wavy nanowires. *Nano Lett.* **2014**, *14*, 3887–3894.

[24] Jiang, X.; Fu, G. T.; Wu, X.; Liu, Y.; Zhang, M. Y.; Sun, D. M.; Xu, L.; Tang, Y. W. Ultrathin AgPt alloy nanowires as a high-performance electrocatalyst for formic acid oxidation. *Nano Res.* **2018**, *11*, 499–510.

[25] Jiang, X.; Liu, Y.; Wang, J. X.; Wang, Y. F.; Xiong, Y. X.; Liu, Q.; Li, N. X.; Zhou, J. C.; Fu, G. T.; Sun, D. M. et al. 1-Naphthol induced Pt_3Ag nanocorals as bifunctional cathode and anode catalysts of direct formic acid fuel cells. *Nano Res.* **2019**, *12*, 323–329.

[26] Khoa, N. T.; Van Thuan, D.; Kim, S. W.; Park, S.; Van Tam, T.; Choi, W. M.; Cho, S.; Kim, E. J.; Hahn, S. H. Facile fabrication of thermally reduced graphene oxide–platinum nanohybrids and their application in catalytic reduction and dye-sensitized solar cells. *RSC Adv.* **2016**, *6*, 1535–1541.

[27] Liu, H.; Ye, F.; Yao, Q. F.; Cao, H. B.; Xie, J. P.; Lee, J. Y.; Yang, J. Stellated Ag-Pt bimetallic nanoparticles: An effective platform for catalytic activity tuning. *Sci. Rep.* **2014**, *4*, 3969.

[28] Mao, H. B.; Feng, J. Y.; Ma, X.; Wu, C.; Zhao, X. J. One-dimensional silver nanowires synthesized by self-seeding polyol process. *J. Nanopart. Res.* **2012**, *14*, 887.

[29] Wang, W.; Wang, Z. Y.; Yang, M. M.; Zhong, C. J.; Liu, C. J. Highly

active and stable Pt (111) catalysts synthesized by peptide assisted room temperature electron reduction for oxygen reduction reaction. *Nano Energy* **2016**, *25*, 26–33.

[30] Daşdelen, Z.; Yıldız, Y.; Eriş, S.; Şen, F. Enhanced electrocatalytic activity and durability of Pt nanoparticles decorated on GO-PVP hybride material for methanol oxidation reaction. *Appl. Catal. B: Environ.* **2017**, *219*, 511–516.

[31] Huang, J.; Liu, Y.; Xu, M. J.; Wan, C. Z.; Liu, H. T.; Li, M. F.; Huang, Z. H.; Duan, X. F.; Pan, X. Q.; Huang, Y. PtCuNi tetrahedra catalysts with tailored surfaces for efficient alcohol oxidation. *Nano Lett.* **2019**, *19*, 5431–5436.

[32] Liu, T. Y.; Li, C. Z.; Yuan, Q. Facile synthesis of PtCu alloy/graphene oxide hybrids as improved electrocatalysts for alkaline fuel cells. *ACS Omega* **2018**, *3*, 8724–8732.

[33] Ren, F. F.; Wang, H. W.; Zhai, C. Y.; Zhu, M. S.; Yue, R. R.; Du, Y. K.; Yang, P.; Xu, J. K.; Lu, W. S. Clean method for the synthesis of reduced graphene oxide-supported PtPd alloys with high electrocatalytic activity for ethanol oxidation in alkaline medium. *ACS Appl. Mater. Interfaces* **2014**, *6*, 3607–3614.

[34] Yazdan-Abad, M. Z.; Noroozifar, M.; Alam, A. R. M.; Saravani, H. Palladium aerogel as a high-performance electrocatalyst for ethanol electro-oxidation in alkaline media. *J. Mater. Chem. A* **2017**, *5*, 10244–10249.

[35] Chung, D. Y.; Lee, K. J.; Sung, Y. E. Methanol electro-oxidation on the Pt surface: Revisiting the cyclic voltammetry interpretation. *J. Phys. Chem. C* **2016**, *120*, 9028–9035.

[36] Zhao, Y. Z.; Li, X. M.; Schechter, J. M.; Yang, Y. Revisiting the oxidation peak in the cathodic scan of the cyclic voltammogram of alcohol oxidation on noble metal electrodes. *RSC Adv.* **2016**, *6*, 5384–5390.

[37] Hofstead-Duffy, A. M.; Chen, D. J.; Sun, S. G.; Tong, Y. J. Origin of the current peak of negative scan in the cyclic voltammetry of methanol electro-oxidation on Pt-based electrocatalysts: A revisit to the current ratio criterion. *J. Mater. Chem.* **2012**, *22*, 5205–5208.

[38] Sulaiman, J. E.; Zhu, S. Q.; Xing, Z. L.; Chang, Q. W.; Shao, M. H. Pt–Ni octahedra as electrocatalysts for the ethanol electro-oxidation reaction. *ACS Catal.* **2017**, *7*, 5134–5141.

[39] Zhang, Y. P.; Gao, F.; Song, P. P.; Wang, J.; Guo, J.; Shiraishi, Y.; Du, Y. K. Glycine-assisted fabrication of N-doped graphene-supported uniform multipetal PtAg nanoflowers for enhanced ethanol and ethylene glycol oxidation. *ACS Sustain. Chem. Eng.* **2019**, *7*, 3176–3184.